Lateral distribution of the muon component in the central region of extensive air showers

1969 J. Phys. A: Gen. Phys. 2 334

(http://iopscience.iop.org/0022-3689/2/3/013)

J. PHYS. A (GEN. PHYS.), 1969, SER. 2, VOL. 2. PRINTED IN GREAT BRITAIN

Lateral distribution of the muon component in the central region of extensive air showers

B. BOŃCZAK†, R. FIRKOWSKI†, J. GAWIN†, J. HIBNER†, R. MAZE‡
J. WDOWCZYK† and A. ZAWADZKI†

† Institute of Nuclear Research, University of Lodz, Poland
‡ Laboratory of Cosmic Physics, Verrieres le Buisson, France

MS. received 4th September 1968, *in revised form 20th November* 1968

Abstract. Using a new device for extensive air shower core localization consisting of four sets of Conversi neon detectors of total area 9 m^2 (comprising 36 000 neon tubes), cores have been located with high accuracy and the lateral muon distribution has been measured for a threshold energy of 0·6 GeV.

50 000 recordings of muon density by means of the Lodz muon analyser have allowed us to obtain a high accuracy of the mean density. The measurements were performed in the central part of extensive air showers: 2 to 30 m from core.

The interpretation of the shape of this distribution is discussed and compared with theoretical calculations. As the muon lateral distribution is mainly determined by the angles of emission of parent pions, some features of the distribution of transverse momenta p_t of pions produced in air can be analysed. For low p_t values a discrepancy is found with the Cocconi empirical p_t distribution which comes from accelerator data. A flattening of the muons' lateral distribution near the shower axis is interpreted as being due to a lack of small p_t values.

1. Introduction

As has been stated by de Beer *et al.* (1966) and Bończak *et al.* (1968), a knowledge of the lateral distribution of the muon component of extensive air showers seems to be of great importance since it enables us to obtain information about some features of the distribution of the transverse momenta of pions produced in collisions with air nuclei, owing to the fact that the muon lateral distribution is mainly determined by the angles of emission of the parent pions. Other factors such as multiple scattering, deflection in the Earth's magnetic field, the transverse momentum of the muon in the pion decay, etc., play a much smaller role. The total deviation of the muon from the axis because of these factors does not exceed 20 per cent of the effect due to the angle of emission of the parent pion. However, before valid conclusions can be drawn, it is essential to perform accurate measurements on the lateral distribution of muons and compare these with theoretical distributions.

The present paper can be considered as a partial contribution to this subject; its main aim is to obtain accurate data on the lateral distribution of muons in the region from 2–30 m from the core. Most of the measurements of the muon lateral distribution performed in the past did not furnish sufficiently accurate information about the distribution in this region since they were usually designed for measurements at larger distances from the core.

Previous work devoted to muon density distributions (Greisen 1960, Nikolski 1962) proceeded from information obtained from arrangements with a large base (values of muon density several tens or several hundreds of metres from the axis). From the data obtained in these experiments it was possible to determine the shape of the radial muon distribution at distances larger than 25 m from the shower axis. This knowledge of the lateral distribution of the muon flux density may be of particular importance since this makes it possible, for instance, to determine the total number of muons in a shower as well as the fluctuations in this number under particular conditions (e.g. constant number of electrons). Extrapolation of the values of the distribution to distances less than 25 m is perhaps allowable, for example, when one is determining the total number of muons, but is impossible when one is trying to utilize the information carried by the muon component in order to obtain data concerning the character of the nuclear collisions.

2. The experimental arrangement

Our experimental device (figure 1) is particularly suitable for measuring the muon lateral distribution not too far from the axis. The apparatus for core location consists of

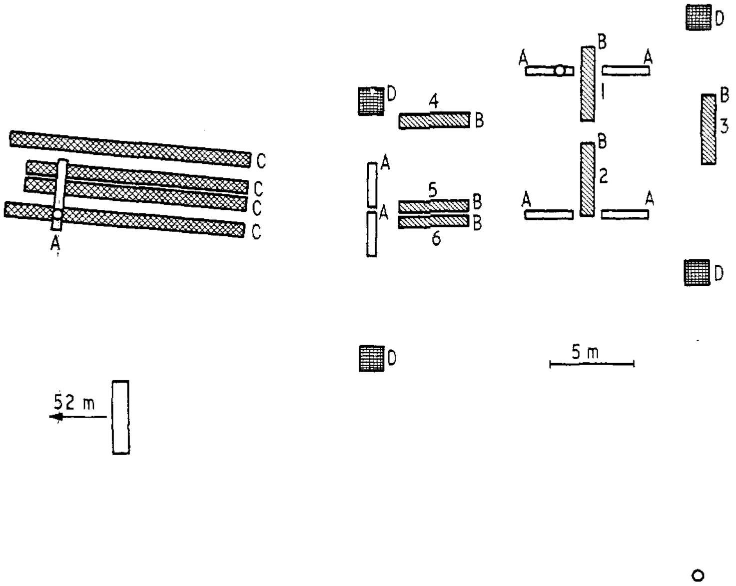

Figure 1. The Lodz experimental arrangement (schematic). A, Geiger–Müller unshielded counters (6·5 m^2 total); B, Geiger–Müller muon detectors 0·6 GeV (21 m^2 total); C, Geiger–Müller muon detectors 5 GeV (42 m^2 total); D, neon flash tubes (9 m^2 total); ○, timing scintillators.

36 000 neon flash tubes covering a total area of 9 m^2 and grouped in four equal sets at the corners of a parallelogram with sides 15 and 20 m. This small separation between the individual detectors ensures accurate determination of the core location. The experimentally evaluated error is 1–2 m at 10 m distance and 3–5 m at 30 m distance (Bończak 1967). It should be noted that the core position is determined for the electromagnetic component of the shower.

The localization of the shower axis is based on the measurement of the density of charged particles in these four trays of the flash-tube hodoscope, assuming the Nishimura–Kamata radial distribution in the Greisen approximation. The accuracy of the procedure was found by the Monte Carlo method, account being taken of the fact that the age parameter s has a value of $s = 1{\cdot}1$ in the central region of the shower.

We have made 50 000 recordings of muon densities by means of the Lodz muon analyser, which has an effective area of 21 m^2 and consists of 152 hodoscoped parts, in order to obtain a high accuracy in the muon flux density. The measurements were performed from 2 m to 30 m from the axis; the threshold energy of the recorded muons was 0·6 GeV (the absorber consists of 30 cm Pb and 12 cm Fe). Showers of all registered angles were used in the analysis, the mean zenith angle being about 26°.

The hodoscoped area was divided into six segments (figure 1, segments 1–6); in this way information about the number of detection elements hit for various distances from the shower axis was obtained.

We introduce the following notation: M, the total number of penetrating component detectors in each segment; m, the number of detectors hit; Δ_p, the density of the penetrating component; S, the area of an individual detector ($S = 0{\cdot}136$ m^2).

3. The elaboration of the experimental data

The whole of the experimental material was divided into 100 sub-groups with definite values of mean shower size $\bar{N}$ and mean core distance $\bar{r}$ (table 1). A histogram of a sub-group is shown in figure 2 as an illustration.

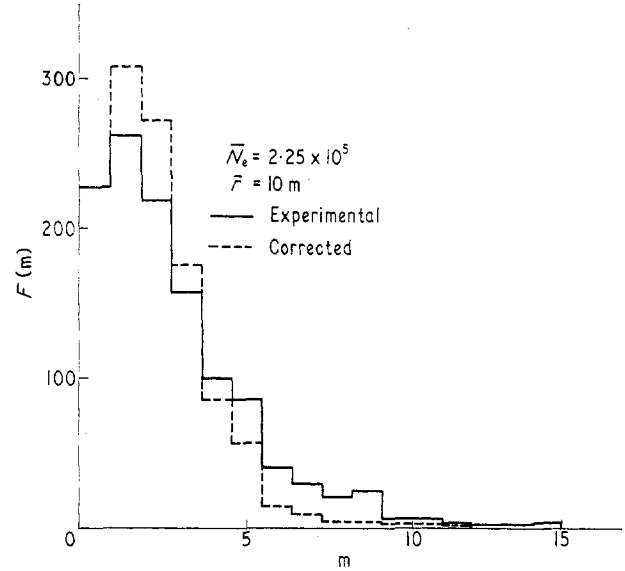

Figure 2. An experimental and corrected histogram corresponding to the mean shower size.

The radial density distribution of the penetrating component was calculated taking into account the effect of multiplication in the absorber (secondary particles of nuclear cascades in the absorber give the appearance of a higher density of the penetrating component).

Each histogram is assigned an averaged value of density in the following manner: the value $m = 0$ has the value $\Delta_p = 0$ assigned to it, while all other values $m < M$ are assigned to the most probable density $\Delta_p = (1/S) \ln\{M/(M-m)\}$.

The weighted mean of these densities is regarded as the averaged density corresponding to the given corrected histogram; the method of correction has been described in detail by Hibner *et al.* (1965).

In accordance with other authors, we assume that the radial density distribution of the penetrating component for distances close to the axis can be described by the relation $\Delta_p = AN_e r^{-n}$. For each group of 10 values of Δ_p associated with each successive value of N_e (table 2), we calculate the coefficients A and n by the least-squares method (table 3). This makes it possible to determine the radial density distribution of the penetrating component corresponding to any value of $\bar{N}_e$. For example, the distribution for $\bar{N}_e = 10^6$, found using a value of the s parameter equal to 1·25, is as shown in figure 3.

The correction for the contribution of the nuclear-active component has been found by two independent methods, as follows.† According to the data of the Bombay group (Chaterjee *et al.* 1963) the number of nuclear-active particles in an extensive air shower at an atmospheric depth of 800 g cm^{-2} is N_N (>1 GeV) = 3100 $(N_e/10^6)^{0\cdot65\pm0\cdot05}$ and falls off to 60 per cent of this value at a depth of 1100 g cm^{-2}. For our depth (1000 g cm^{-2}) we take a coefficient of 0·73. Assuming an energy threshold of 2 GeV for nuclear-active particles from the energy spectrum of Greisen (1960), we find the intensity to be 0·63 of the former.

† One should distinguish the procedure of subtracting the nuclear-active component from the total penetrating component and the above described corrections for multiplications in the absorber. The later corrections give densities of the total penetrating component on the basis of the histograms of the shielded detectors hit.

Table 1. 100 sub-groups of recorded showers with definite values of mean shower size and mean core distance

r (m) \ $\bar{N}_e$	$1 \cdot 15 \times 10^5$	$2 \cdot 25 \times 10^5$	$3 \cdot 05 \times 10^5$	$3 \cdot 65 \times 10^5$	$4 \cdot 05 \times 10^5$	$4 \cdot 55 \times 10^5$	$5 \cdot 15 \times 10^6$	$6 \cdot 35 \times 10^5$	$8 \cdot 65 \times 10^5$	$2 \cdot 1 \times 10^6$
2	734	470	261	115	100	83	58	129	88	67
4	1171	877	474	195	128	168	104	205	175	95
6	1245	1031	655	259	207	211	162	236	217	204
8	1204	1144	847	316	268	319	227	392	283	246
10	1138	1166	898	418	333	350	257	472	365	318
12	922	1020	862	373	255	375	279	520	381	336
14	779	1006	951	446	397	432	386	700	619	530
17	502	975	1044	522	427	585	493	1012	884	810
21	166	297	512	316	293	450	425	972	938	1036
26	69	100	147	113	146	221	276	756	1134	1661

Table 2. The values of Δ_p associated with the successive values of $\bar{N}_e$

r (m) \ $\bar{N}_e$	$1 \cdot 15 \times 10^5$	$2 \cdot 25 \times 10^5$	$3 \cdot 05 \times 10^5$	$3 \cdot 65 \times 10^5$	$4 \cdot 05 \times 10^5$	$4 \cdot 55 \times 10^5$	$5 \cdot 15 \times 10^5$	$6 \cdot 35 \times 10^5$	$8 \cdot 65 \times 10^5$	$2 \cdot 1 \times 10^6$
2	1·222	1·553	2·166	2·321	2·717	2·398	—	3·988	3·895	—
4	0·958	1·176	1·561	1·723	2·165	1·865	1·731	2·874	2·859	—
6	0·726	0·943	1·117	1·378	1·312	1·597	1·795	2·306	2·434	4·741
8	0·613	0·802	1·151	1·057	1·037	1·382	1·467	1·704	2·254	4·073
10	0·472	0·680	0·814	0·866	0·955	1·152	1·145	1·371	1·871	3·381
12	0·466	0·559	0·683	0·814	0·745	1·010	1·112	1·205	1·512	3·129
14	0·438	0·484	0·608	0·697	0·719	0·807	0·889	1·036	1·390	2·436
17	0·450	0·486	0·508	0·602	0·579	0·700	0·806	0·896	1·152	2·169
21	0·404	0·376	0·435	0·550	0·547	0·613	0·607	0·760	0·931	1·763
26	0·812	0·384	0·436	0·438	0·495	0·546	0·571	0·668	0·828	1·630

Table 3. The values of the A and n coefficients corresponding to the successive values of $\bar{N}_e$

$\bar{N}_e$	$1 \cdot 15 \times 10^5$	$2 \cdot 25 \times 10^5$	$3 \cdot 05 \times 10^5$	$3 \cdot 65 \times 10^5$	$4 \cdot 05 \times 10^5$	$4 \cdot 55 \times 10^5$	$5 \cdot 15 \times 10^5$	$6 \cdot 35 \times 10^5$	$8 \cdot 65 \times 10^5$	$2 \cdot 1 \times 10^6$
A	1·811	2·716	4·332	4·309	4·972	5·117	6·287	8·110	8·618	9·423
n	0·523	0·618	0·735	0·685	0·736	0·683	0·737	0·772	0·712	0·770

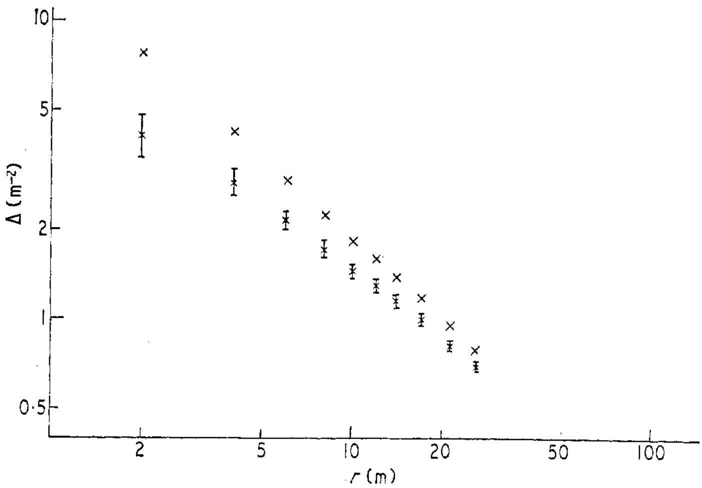

Figure 3. × the radial distribution of the penetrating particle flux for $\bar{N}_e = 10^6$, using the value of the s parameter equal to 1·25. ⫯ the radial distribution of the muon flux.

If, after Cocconi (1961) and Nikolski *et al.* (1956), we assume that the radial density distribution of nuclear-active particles has the shape $\Delta_N \sim r^{-1 \cdot 4}$ we obtain the values given in table 4. The table also lists the values stemming from the distribution obtained by Hibner (1964) (the third column).

Table 4. The radial density distribution of nuclear-active particles obtained using the data of Chaterjee *et al.* (1964)(second column) and of Hibner (1964) (third column)

r (m)	$\bar{N}_e = 10^6$	$\bar{N}_e = 10^6$
2	3·67	3·36
4	1·39	1·28
6	0·79	0·72
8	0·53	0·48
10	0·39	0·35
12	0·30	0·27
14	0·24	0·22
17	0·18	0·17
21	0·14	0·13
26	0·10	0·09

The radial density distribution of the muon flux obtained after subtraction of the nuclear-active component is also shown in figure 3. It should, therefore, be stressed here that the experimental distribution represents the pure muonic component.

The indicated errors are mainly caused by the various corrections—the errors of the initial distributions being practically negligible.

As was mentioned above, we assume the age parameter $s = 1 \cdot 25$ for the evaluation of the shower size. However, work, as yet unpublished, which has been carried out at Lodz shows that the value of the parameter s in the central part of the extensive air shower is 1·1 instead of 1·25. This markedly changes the value of $\bar{N}_e$; taking this into consideration the radial distribution of the muon density is related to the shower size $\bar{N}_e = 8 \cdot 2 \times 10^5$ and not 10^6. When the corrections ensuing from this are taken into account, the radial density distribution of the muon flux for a shower of size $N_e = 10^6$ is as shown in figure 4.

In the interval from 10 to 20 m, we find good agreement with other results. The ratio of the respective values of the muon density obtained by Trümper *et al.* (1968, private communication) to those in the Lodz experiments for r = 10–15 and 20 m are, respectively,

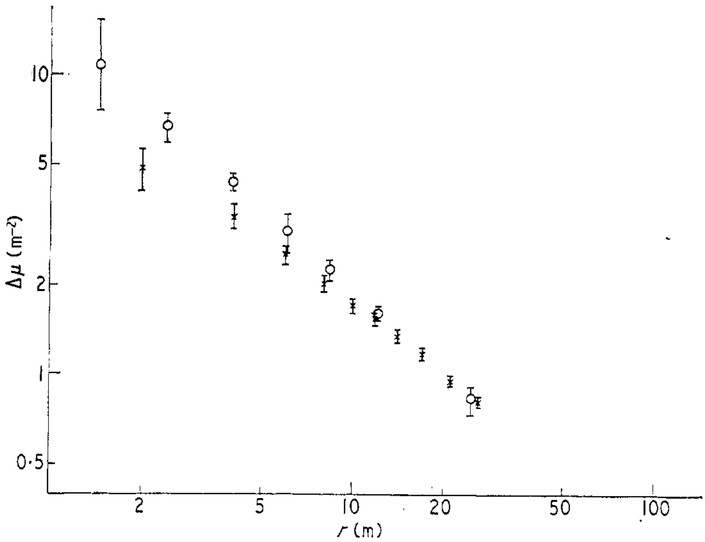

Figure 4. The radial distribution of the muon flux, after correction of the $\bar{N}_e$ value; ⫯ present work; ⫯ Trümper *et al.* (1968).

1·08–1·03 and 1·00. The less pronounced flattening for smaller values of r obtained by Trümper *et al.* and by Chaterjee *et al.* (1964) is, in our opinion, due to the fact that the contribution of the nuclear-active component had not been fully taken into account.

4. Conclusions

The present experimental results have been compared with the theoretical calculations of de Beer *et al.* (1966). These authors assumed the CKP distribution (Cocconi *et al.* 1961) of transverse momentum and performed the calculations for two variants: (i) the complete transverse momentum distribution; (ii) a distribution with a cut-off applied so that pions with transverse momenta below 0·1 GeV/c were suppressed.

Figure 5 represents both theoretical curves; the upper one corresponds to the full p_t distribution, the lower one to the distribution with a cut-off at 0·1 GeV/c. The points represent our experimental results.

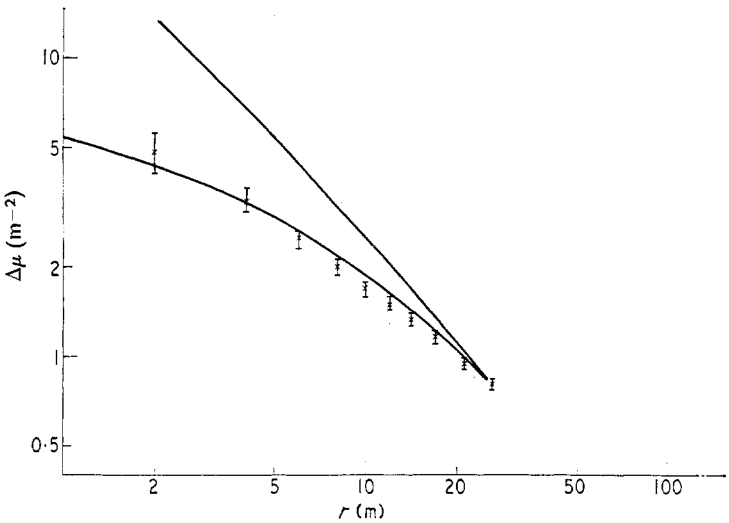

Figure 5. The experimental density distribution of the muon flux (present work) in comparison with the theoretical curves; the upper curve corresponds to the full p_t distribution, the lower to the distribution with a cut-off at 0·1 GeV/c.

In conclusion it should be pointed out that the muon lateral distribution is flattened at small distances from the core. This seems to provide some indication of a lack of particles with low p_t among the secondary pions produced in pion–light-nuclear collisions. Specifically it can be seen (figure 5) that there is good agreement between the experimental distribution and theoretical one with p_t values below 0·1 GeV/c suppressed. This can be considered as an indication of a lack, as distinct from a complete absence, of low transverse momenta. It should be noted that in the case of a higher mean transverse momentum the relative lack of low transverse momentum would be observed even if the shape of the distribution remained of the form: $p_t \exp(p_t/p_0)$.

Acknowledgments

The authors are very indebted to Professor A. W. Wolfendale for many interesting discussions. Our thanks are also due to Mrs. L. Bończak for her contribution in the treatment of the data.

References

DE BEER, J. F., HOLYOAK, B., WDOWCZYK, J., and WOLFENDALE, A. W., 1966, *Proc. Phys. Soc.*, **89**, 567–85.
BOŃCZAK, B., 1967, *Ph.D. Thesis*, University of Lodz.
BOŃCZAK, B., *et al.*, 1968, *Can. J. Phys.*, **46**, S102–3.
CHATERJEE, B. K., *et al.*, 1964, *Proc. 8th Int. Conf. on Cosmic Rays, Jaipur*, 1963, Vol. 4 (Bombay : Commercial Printing Press), pp. 227–43.
COCCONI, G., 1961, *Handb. Phys.*, **46/1**, 215–56 (Berlin : Springer-Verlag).
COCCONI, G., KOESTER, A., and PERKINS, D. H., 1961, *Lawrence Rad. Lab. Rep.*, UCID-1444.
GREISEN, K., 1960, *Ann. Rev. Nucl. Sci.*, **10**, 63–108.
HIBNER, J., 1964, *Ph.D. Thesis*, University of Lodz.
HIBNER, J., GAWIN, J., WDOWCZYK, J., and ZAWADZKI, A., 1965, *Acta Phys. Pol.*, **27**, 681–705.
NIKOLSKI, S. I., 1962, *Usp. Fiz. Nauk*, **7**, 365–408.
NIKOLSKI, S. I., WAWILOW, I. N., and BATOW, W. N., 1956, *Dokl. Akad. Nauk SSSR*, **111**, 71–3.